LIDAR MEASUREMENTS OF TROPOSPHERIC OZONE IN THE ARCTIC

Jeffrey Seabrook and James Whiteway

Centre of Research in Earth and Space Science, York University, Toronto, Ontario, M3J 1P3
Email: whiteway@yorku.ca

ABSTRACT

This paper reports on differential absorption lidar (DIAL) measurements of tropospheric ozone in the Canadian Arctic during springtime. Measurements at Eureka Weather Station revealed that mountains have a significant effect on the vertical structure of ozone above Ellesmere Island. Ozone depletion events were observed when air that had spent significant time near to the frozen surface of the Arctic Ocean reached Eureka. This air arrived at Eureka by flowing over the surrounding mountains. Surface level ozone depletions were not observed during periods when the flow of air from over the sea ice was blocked by mountains. In the case of blocking there was an enhancement in the amount of ozone near the surface as air from the mid troposphere descended in the lee of the mountains. Three case studies will be shown in the presentation, while one is described in this paper.

1. INTRODUCTION

Lidar systems for tropospheric ozone measurements have been developed at York University for field deployment. One was installed on the Canadian Coast Guard Icebreaker Ship Amundsen [1] and on the Polar-5 (DC-3) aircraft [2] for studies of air chemistry over Arctic sea ice. Another lidar for ground-based measurements of tropospheric ozone was constructed for the Canadian Network for the Detection of Atmospheric Change (CANDAC) and installed as part of the Polar Environment Atmospheric Research Laboratory (PEARL) at Eureka Weather Station on Ellesmere Island in the Canadian Arctic. The lidar was installed in 2007 and operated for several intensive periods until 2012.

The measurement campaigns over sea ice have focused on surface level ozone depletion events (ODEs) that are well known to occur during springtime in the Arctic [3,4,5]. The ozone depletion has been explained as being caused by Bromine atoms that originate from photochemical reactions on snow and fresh sea ice surfaces [6]. The aircraft and ship based lidar measurements over the sea ice have found that the ODEs extend from the surface to heights of a few hundred meters [1,2]. Analyses of air trajectories revealed that ozone depleted air spent significant time in the surface layer over the frozen ocean surface and open leads [1,2].

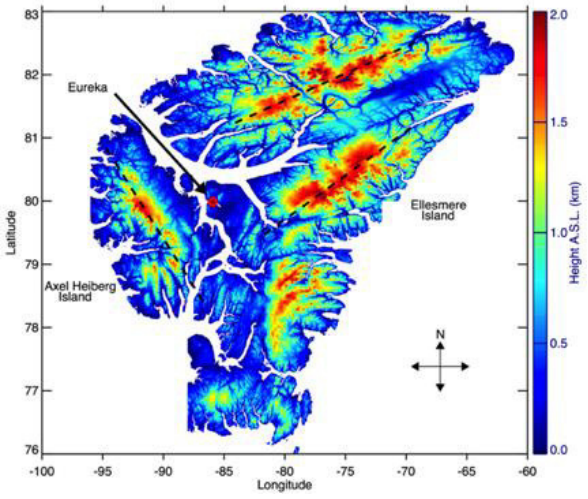

Figure 1. Map of topography in the vicinity of Eureka Weather Station on Ellesmere Island.

The current study primarily concerns ground based lidar measurements of tropospheric ozone over Eureka Weather Station on Ellesmere Island. Figure 1 shows the topography of Ellesmere Island and Axel Heiberg Island, with Eureka indicated on the map at 80° N, 85° W. Air from over the sea ice interacts with various mountain ranges to the west, southeast, east and northeast before it reaches Eureka. It was found that traversal of these mountain ranges had a significant effect on the vertical structure of ozone measured above Eureka. One case study will be

presented that involved significant changes in the height distribution of ozone in the lower troposphere over a 6-day period. The observations are interpreted using back trajectory analysis and this has provided an illustration of the effect of mountains on the amount of near surface ozone over land in the Arctic.

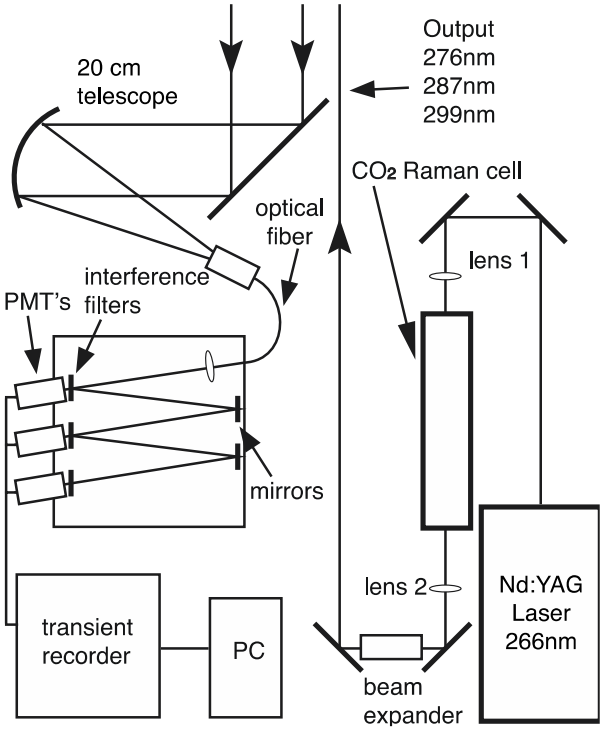

Figure 2. Schematic diagram of the differential Absorption Lidar (DIAL) at Eureka

2. METHOD

The ground based Differential Absorption Lidar (DIAL) instrument used for this study had a design that was essentially equivalent to the system employed for previous ship and aircraft based studies of ozone over sea ice [1,2]. A schematic diagram of the lidar is shown in Fig. 2. The fourth harmonic of a Q-switched Nd:YAG laser (266 nm, 70 mJ per pulse, 20 Hz repetition rate) was focused into a gas cell filled with 140 PSI of CO_2 to generate pulsed light at wavelengths of 276 nm, 287 nm and 299 nm by stimulated Raman scattering [7] and then directed into the atmosphere along the zenith. Backscattered light was collected with a 20 cm off axis parabolic mirror and a 1.5 mm diameter optical fiber positioned in the focal plane, 500 mm from the mirror, to form a receiver field of view of 3.0 mrad. Full overlap between the emitted laser pulse and the telescope field of view occurred at a range of approximately 250 m and the signal received from below that height was not used in the ozone analysis. The three wavelengths (276, 287, and 299 nm) were separated in the receiver using the transmittance and reflectance from interference filters having a bandwidth of 1 nm and tilted at an angle of 5 degrees. The backscatter signals were detected using photomultipliers to generate electrical signals that were recorded using photon counting for the weak signals from distances greater than 1.8 km (typically) and using analog to digital conversion for the strong signals in the near range. The raw data was recorded with a range gate of 7.5 m and an integration period of 1200 laser shots (1 min). During data processing the recorded backscatter signal profiles were averaged both spatially and temporally in order to reduce the measurement uncertainty. The 276/287 nm analog signals were used below a height of 1.8 km and the 287/299 nm photon counting signals were used at greater heights (depending on signal strength).

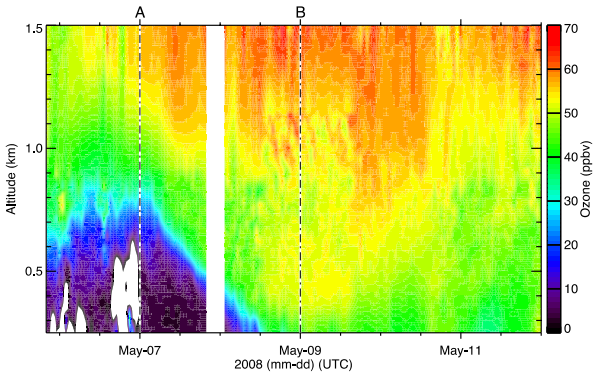

Figure 3. Contour plot of lidar ozone measurements during the period from May 6th to 12th, 2008.

3. OBSERVATIONS AND ANALYSIS

One case will be presented here that illustrates the influence of the surrounding topography on the vertical distribution of ozone. Figure 3 shows a contour of the lidar measurements of ozone vertical distribution during the 6-day period from the 6th to 12th of May in 2008. There was a surface level ozone depletion event (ODE) that extended to a height of 800 m on May 7th when the volume

mixing ratio of ozone decreased to less than 10 ppb. The ODE was then replaced after 9 May by air with enhanced ozone content of 60 ppb (in comparison with the background of 40 ppbv) that descended from greater heights.

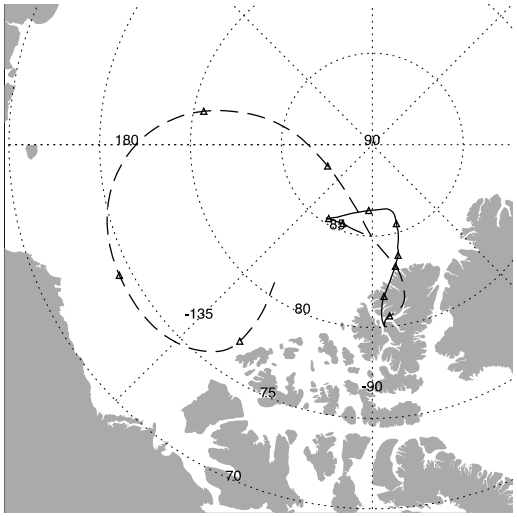

Figure 4. Back trajectories of air arriving at Eureka at a height of 300m above sea level on May 7th (solid) and May 9th (dashed).

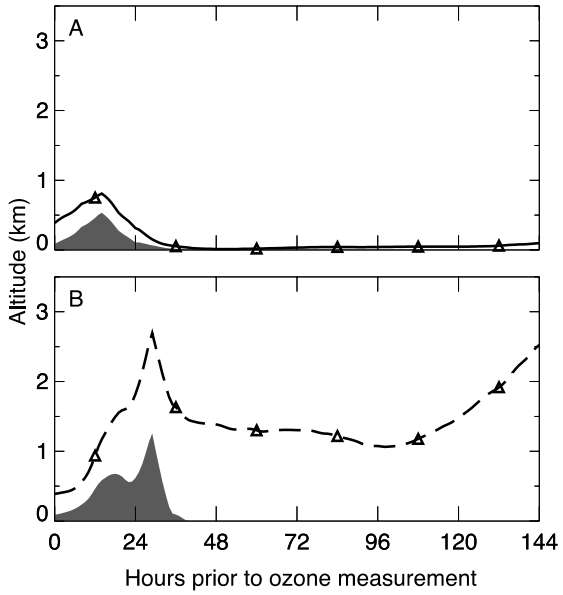

Figure 5. Height along the back trajectories shown in Fig 4 for May 7th (solid) and May 9th (dashed). The shaded region indicates the height of the topography beneath the air trajectory.

The back trajectories for air arriving above Eureka were calculated with the HYSPLIT model [8]. These are shown in terms of geographical position in Fig. 4 for May 7th, when there was an ozone depletion, and for May 9th, when there was an ozone enhancement (points A and B in Fig. 3). In each case the air originated from over the frozen Arctic Ocean. The reason for the transition from ozone depleted air to the ozone enhancement is apparent in Fig. 5, which shows the height along the calculated back trajectories. The air arriving over Eureka on May 7th had spent significant time in contact with sea ice during the previous 6 days. It traversed the mountains on Ellesmere Island prior to arriving at Eureka. The air that was arriving above Eureka on May 9th was not in contact with the surface of the frozen Arctic Ocean during the previous 6 days. This air had descended from heights above 2 km in the lee of the mountains northeast of Eureka.

4. INTERPRETATION

When air near the surface blows inland from the ocean it can flow over a mountain range if the wind speed is sufficient that there is enough kinetic energy to overcome the force of buoyancy and the associated change in potential energy. If the wind speed is too slow it will not be able to flow over the mountain. For an extended mountain range the flow will be blocked and replaced by air flowing down from greater heights on the lee side of the mountains. In this simplified analysis the conditions for flow over the mountain, or blocking, can be differentiated with the Froude number, Fr = U/Nh, where U is the wind speed perpendicular to the axis of the mountain range, N is the buoyancy frequency, and h is the change in height required for air to flow over the mountains. The Froude number is the square root of the ratio of kinetic energy to the change in potential energy. When Fr < 1 the airflow will be blocked by the mountains, and when Fr > 1 the flow will pass over the mountains [9]. The flow conditions determine whether the air at the surface in the lee of the mountains is originating from the sea ice surface, and thus ozone depleted, or from the free troposphere with greater ozone concentration.

The Froude number was calculated using the wind and temperature profiles from the HYSPLIT model at a position on the back trajectories that was upwind of the mountains. For air that was

arriving at Eureka during the ozone depletion on May 7th the Froude number upwind of the mountains was 1.30. As this is greater than unity, the wind speed near the sea ice surface was large enough to flow over the mountains. Previous observations have found that air that spends significant time in contact with the sea ice surface is depleted in ozone. This explains why the air that arrived at Eureka on May 7th was depleted in ozone.

The Froude number upwind of the mountains had a value of 0.11 for the air arriving over Eureka on May 9th. With a Froude number less than unity, the flow from over the sea ice was blocked by the mountains. The compensating descent in the lee of the mountains brought air from heights above 2 km with greater ozone content.

5. CONCLUSION

A differential absorption lidar (DIAL) for measurements of tropospheric ozone was operated at Eureka Weather Station on Ellesmere Island in the Canadian Arctic. Large variations in the vertical distribution of ozone were observed during spring that are associated with surface level ozone depletion events over sea ice and the effects of mountains on atmospheric flow patterns.

ACKNOWLEDGEMENTS

This work was carried out as part of the Canadian Network for the Detection of Atmospheric Change (CANDAC). Funding was provided by the Canadian Natural Sciences and Engineering Research Council (NSERC) Discovery program, the NSERC International Polar Year (IPY) Program, the Canadian Foundation for Climate and Atmospheric Sciences (CFCAS), and the Canadian Foundation for Innovation (CFI).

REFERENCES

[1] Seabrook, J., J. Whiteway, J., R. Staebler, J. Bottenheim, L. Komguem, L. Gray, D. Barber, and M. Asplin, 2011: LIDAR measurements of Arctic boundary layer ozone depletion events over the frozen Arctic Ocean, *J. Geophys. Res.*, **116,** doi:10.1029/2011JD016335.

[2] Seabrook, J., J. Whiteway, L. Gray, R. Staebler, A. Herber, 2013: Airborne lidar measurements or surface ozone depletion over Arctic sea ice, *Atmos. Chem. Phys.,* **13**, 1 – 7.

[3] Oltmans, S. and W. Komhyr, 1986: Surface ozone distributions and variations from 1973-1984 measurements at the NOAA geophysical monitoring for climatic change baseline observatories, *J. Geophys. Res.*, **91**, 5229 – 5236.

[4] Bottenheim, J., A. Gallant, and K. Brice, 1986: Measurements of NOy species and O3 at 82 N latitude, *Geophys. Res. Lett.*, **13**, 113 – 116.

[5] Barrie, L., J. Bottenheim, R. Schnell, P. Crutzen, and R. Rasmussen, 1988: Ozone destruction and photochemical reactions at polar sunrise in the lower Arctic atmosphere, *Nature*, 334, 138 – 141.

[6] Simpson, W.R. et al., 2007: Halogens and their role in polar boundary-layer ozone depletion, *Atmos. Chem. Phys.*, **7**, 4375 – 4418.

[7] Nakazato, M., T. Nagai, T. Sakai, Y. Hirose, 2007: Tropospheric ozone differential-absorption lidar using stimulated Raman scattering in carbon dioxide, *Appl. Opt.*, **46**, 2269 – 2279, doi:10.1364/AO.46.002269.

[8] Draxler, R. and G. Hess, 1998: An overview of the HYSPLIT 4 modeling system for trajectories, dispersion, and deposition, *Australian Meteorological Magazine*, **47**, 295 – 308.

[9] Wang, C., G. Chen, 2003: On the formation of leeside mesolows under different Froude number flow regime in TAMEX, *J. Met. Soc. Japan,* **81**, 339 – 365.